Article

Chinese Science Bulletin

Geochemistry

October 2013 Vol.58 No.28-29: 3564–3579
doi: 10.1007/s11434-013-5904-1

A ~2.5 Ga magmatic event at the northern margin of the Yangtze craton: Evidence from U-Pb dating and Hf isotope analysis of zircons from the Douling Complex in the South Qinling orogen

HU Juan[1], LIU XiaoChun[1*], CHEN LongYao[1], QU Wei[1], LI HuaiKun[2] & GENG JianZhen[2]

[1] *Institute of Geomechanics, Chinese Academy of Geological Sciences, Beijing 100081, China;*
[2] *Tianjin Center of China Geological Survey, Tianjin 300170, China*

Received December 28, 2012; accepted May 8, 2013; published online May 22, 2013

The poorly studied Douling Complex is a crystalline basement that developed in the Neoproterozoic-Paleozoic weakly metamorphosed to non-metamorphosed strata at the South Qinling tectonic belt. Five banded dioritic-granitic gneiss samples from the Douling Complex were chosen for LA-MC-ICPMS U-Pb zircon dating, which yielded protolith emplacement ages of 2469 ± 22 Ma, 2479 ± 12 Ma, 2497 ± 21 Ma, 2501 ± 17 Ma and 2509 ± 14 Ma, respectively. An important peak age of ~2.48 Ga was also obtained for a metasedimentary rock in the same region. These discoveries suggest the occurrence of magmatic activity of 2.51–2.47 Ga at the northern margin of the Yangtze craton. The age-corrected $\varepsilon_{Hf}(t)$ values obtained from *in situ* zircon Hf isotopic analysis are mainly between −5.5 and +0.3, and the two-stage zircon Hf model ages range from 3.30 to 2.95 Ga. Considering two important periods of ~3.3–3.2 Ga and ~2.95–2.90 Ga for the continental crustal growth in the Yangtze craton, we infer that the dioritic-granitic gneisses from the Douling Complex are the products of reworking of Paleo- to Mesoarchean crust at the northern margin of the Yangtze craton at ~2.5 Ga. In addition, metamorphic ages of 837 ± 8 Ma and 818 ± 10 Ma were obtained for zircon overgrowth rims from a dioritic gneiss and a metasedimentary rock, indicating that the main phase amphibolite facies metamorphism of the Doulng Complex occurred during the Neoproterozoic, although its geological meaning remains ambiguous.

U-Pb zircon geochronology, Hf isotope, latest Neoarchean, magmatic event, Douling Complex, Yangtze craton

Citation: Hu J, Liu X C, Chen L Y, et al. A ~2.5 Ga magmatic event at the northern margin of the Yangtze craton: Evidence from U-Pb dating and Hf isotope analysis of zircons from the Douling Complex in the South Qinling orogen. Chin Sci Bull, 2013, 58: 3564–3579, doi: 10.1007/s11434-013-5904-1

The North China and Yangtze cratons are the two largest Precambrian basement blocks in China, which collided along the Qinling-Tongbai-Dabie-Sulu orogenic belt during the late Permian to Triassic [1]. It is well known that Archean rocks are extensively exposed in the North China craton. The oldest rocks and crustal materials were dated at 3.8 Ga. Two major phases of magmatism occurred in 2.8–2.7 Ga and 2.55–2.50 Ga, whereas high grade metamorphism took place at ~2.5 Ga [2,3]. In contrast, the Precambrian basement of the Yangtze craton is poorly exposed; it was deeply buried and was covered by voluminous Neoproterozoic-Phanerozoic sedimentary sequences. The growing amount of isotopic age data from Archean to Paleoproterozic, particularly the recently published U-Pb zircon ages, has led many researchers to suggest that Archean crystalline basement is widespread beneath the Yangtze craton [4]. However, the supporting evidence mainly comes from U-Pb studies of detrital zircons in metasedimentary rocks [5–9] or inherited zircons in igneous rocks [10–14]. The Archean age information obtained for the exposed basement rock series are mostly from the Kongling high grade metamorphic terrane at the northern margin of the Yangtze craton [15–20], with sporadic reports from the granulites in the Yudongzi Group and the Dabie Mountains [21–23]. To date, three main episodes of Archean magmatic event in the Yangtze craton have been recognized, i.e. at approximately 3.3–3.2 Ga, 2.95–2.9 Ga and 2.7–2.6 Ga, respectively [3,20].

*Corresponding author (email: liuxchqw@yahoo.com.cn)

The Qinling orogen marks a convergence zone separating the North China craton from the Yangtze craton. It has experienced different tectonic stages and formed a composite continental orogenic belt through different tectonic regimes [24]. Understanding the nature of the main tectonic units of the Qinling orogen is important not only for recognizing the amalgamation process between the North China and Yangtze cratons during the Phanerozoic, but also for elucidating the formation and evolution of Precambrian continental crust. Although the tectonic nature of the North Qinling tectonic belt is still unclear, it is generally accepted that the South Qinling tectonic belt was derived from the Yangtze craton basement [25,26]. Therefore, the South Qinling tectonic belt is also an important venue for unraveling the early tectonic evolution of the Yangtze craton. The Douling Complex represents a crystalline basement developed in the Neoproerozoic-Paleozoic weakly metamorphosed to non-metamorphosed strata in the South Qinling tectonic belt. This complex only experienced amphibolite facies metamorphism [27,28] and never underwent HP/UHP metamorphism. Due to inadequate geochronological research and inaccurate age data [29,30], no conclusive results could be drawn yet regarding the protolith and metamorphic ages of this complex, and the comparison between this complex and the HP/UHP metamorphic terrane located at the same tectonic position still remains unclear. In this contribution, different rock types of the Douling Complex were conducted by LA-MC-ICPMS U-Pb zircon dating and Hf isotope analysis. The banded dioritic-granitic gneisses gave evidence of magmatism at ~2.5 Ga. This discovery is very important for discussing the tectonic evolution of the Yangtze craton during the late Archean to early Paleoproterozoic.

1 Regional geology

The Douling Complex (also called the Douling Group) is located at the South Qinling tectonic belt to the southern side of the Shangdan Fault. It occured as lenticular body in NWW-SEE direction. This complex is separated from the Neoproterozoic Wudang Group by a ductile shear zone in the south and from the Devonian Liuling Group by fault contact in the north. The exposure area of this complex is less than 500 km^2, where was intruded by voluminous intermediate to felsic intrusives during the Neoproterozoic (Figure 1). The Douling Complex is mainly composed of banded dioritic-granitic gneiss (including amphibole-plagioclase gneiss, biotite-plagioclase gneiss, plagioclase gneiss and two-feldspar gneiss) with intercalated calc-silicate rock, amphibolite and marble, where the amphibolite sometimes interbeds with gneiss. Using conventional thermobarometers, the metamorphic conditions are determined to be 650–700°C and 0.70–0.87 GPa [27,28], which are equivalent to upper amphibolite facies conditions. However, the amphibolite mineral assemblage was commonly overprinted by greenschist facies metamorphism. Neoproterozoic intrusives mainly consist of diorite, granodiorite and granite of 735–705 Ma [28] (our unpublished data), which are generally subjected to late deformation.

Geochronology studies on the Douling Complex are few. The age of 1878 ± 256 Ma has been obtained for five felsic gneiss samples using whole-rock Sm-Nd isochron method [29], which is distinctly different from the ages of 1635 ± 22 Ma and 1672 ± 25 Ma obtained for a gneiss by single zircon grain evaporation method. Thus, the protolith age of the gneisses from the Douling Complex remains uncertain.

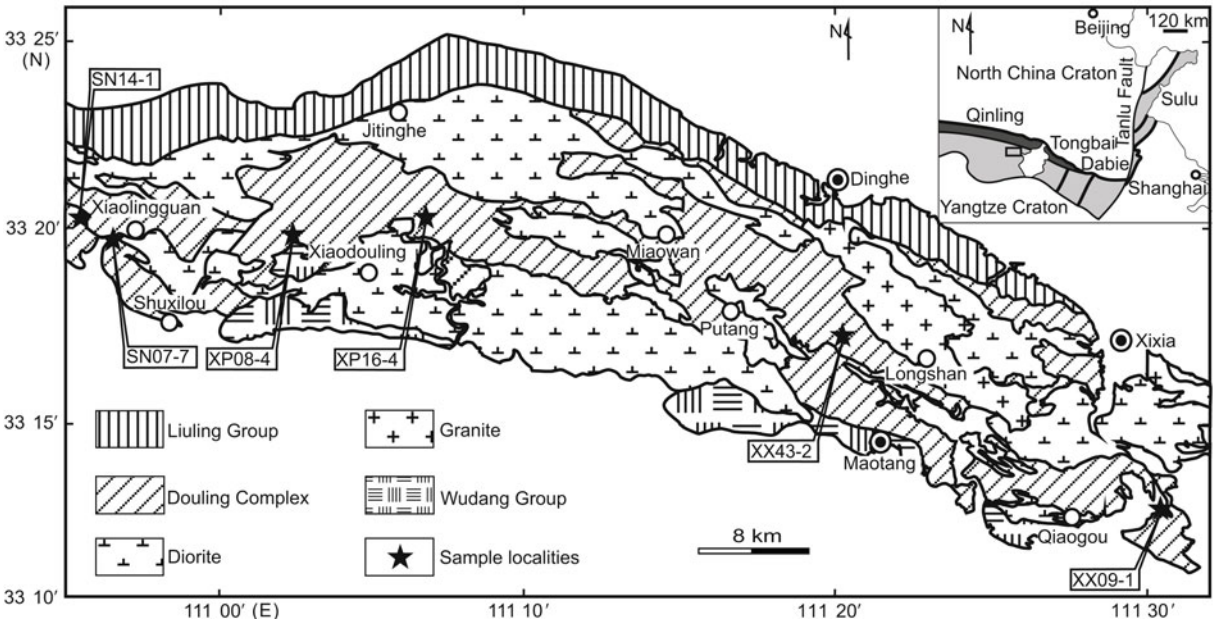

Figure 1 Simplified geological map of the Douling Complex in the South Qinling tectonic belt. The sampling localities of the studied rocks are indicated.

Zhang et al. [30] examined calc-silicate rocks from the Douling Complex using SHRIMP U-Pb zircon and Sm-Nd dating. They obtained the remnant zircon ages of 2.6–2.5 Ga and the Nd model ages of 2.76–2.67 Ga, which further indicated the possible presence of Neoarchean crustal materials in the Douling Complex. In addition, the metamorphic zircons from calc-silicate rocks gave ages of ~1.95 Ga and 834 ± 31 Ma. The high and low temperature $^{40}Ar/^{39}Ar$ plateau ages of amphibole were 833 ± 17 Ma and 323 ± 8 Ma, respectively. Whole-rock Rb-Sr isochron age of 422 ± 16 Ma was also obtained for a gneiss. Hence, the Douling Complex were inferred to comprise lithostratigraphic units with different ages and source regions and may have been affected by multi-phase metamorphism during the Paleoproterozoic, Jinningian, and late Caledonian-Hercynian [28−30].

2 Samples and analytical procedures

2.1 Samples

In order to precisely determine the protolith ages of metaigneous and metasedimentary rocks from the Douling Complex, six representative samples including five dioritic-granitic gneisses (samples XX09-1, XX43-2, XP08-4, XP16-4 and SN07-7) and one metapelite (sample SN14-1) were chosen for LA-MC-ICPMS U-Pb zircon dating. Except for sample XX09-1 that showed substantial Pb loss in zircon, four gneisses were also carried out Hf isotopic analysis on magmatic zircon domains. All selected rocks experienced amphibolite facies metamorphism followed by various degrees of overprinting by the greenschist facies metamorphism. Their geographic coordinates, mineral assemblages and age results are presented in Table 1.

Dioritic-granitic gneisses mainly consist of amphibole-plagioclase gneiss, biotite-plagioclase gneiss, plagioclase gneiss and two-feldspar gneiss. All these rocks are fine-grained and banded, commonly intercalated with thin layers or bands of amphibolites (Figure 2(a)). The rocks are commonly composed of plagioclase, K-feldspar, quartz and opaque minerals. Some intermediate rocks contain amphibole, whereas felsic rocks contain biotite or are enriched in K-feldspar. The overprinting of late greenschist facies metamorphism and deformation are distinct and led to a

Table 1 Sampling localities, mineral assemblages and age results of the dated rocks from the Douling Complex

Sample	Location	Coordinates	Lithology	Mineral assemblage[a)]	Age (Ma)
XX09-1	Dangziling	33°12′30″N 111°30′10″E	amphibole-plagioclase gneiss	Amp + Pl + Kfs + Qtz + Oq; Secondary: Ser + Ep	2469 ± 22 837 ± 8
XX43-2	Xijiucaogou	33°16′38″N 111°20′06″E	amphibole-plagioclase gneiss	Amp + Pl + Qtz + Oq; Secondary: Chl + Ep	2479 ± 12
XP08-4	Dadouling	33°19′40″N 11°02′35″E	plagioclase gneiss	Pl + Kfs + Qtz + Oq; Secondary: Ser + Chl + Ep	2497 ± 21
XP16-4	Shizigou	33°20′15″N 111°06′37″E	two-feldspar gneiss	Pl + Kfs + Qtz + Oq; Secondary: Ser + Chl + Ep	2501 ± 17
SN07-7	Xiaolingguan	33°19′43″N 110°56′31″E	biotite-plagioclase gneiss	Bt + Pl + Kfs + Qtz + Qq; Secondary: Ser + Chl + Ep	2616 ± 11 2509 ± 14
SN14-1	Shifanggou	N 33°20′17″E 110°55′30″	metapelite	Grt + Bt + Sill + Ky + St + Pl + Qtz + Rt + Ilm; Secondary: Chl	3032–1362 818 ± 10

a) Amp, Amphibole; Bt, biotite; Chl, chlorite; Ep, epidote; Grt, garnet; Ilm, ilmenite; Kfs, K-feldspar; Ky, kyanite; Oq, opaque minerals; Pl, plagioclase; Qtz, quartz; Rt, rutile; Ser, sericite; Sill, sillimanite; St, staurolite.

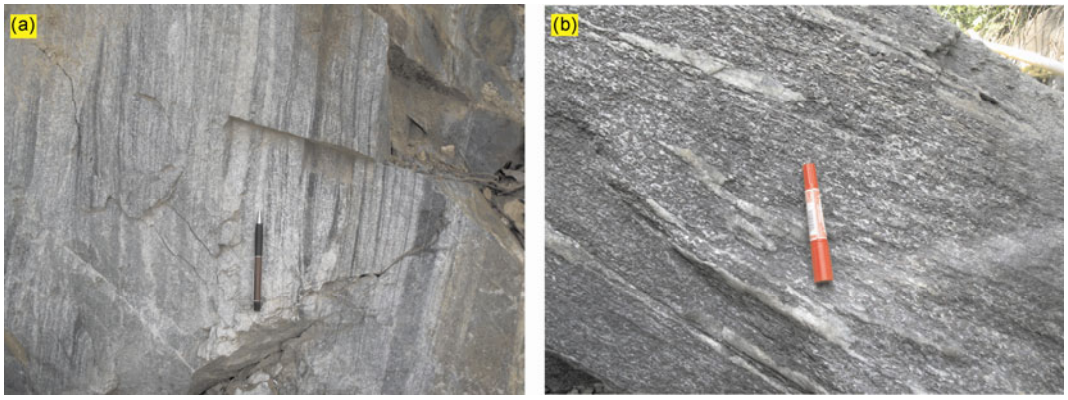

Figure 2 Photographs showing the field occurrences of the dated rocks. (a) Banded amphibole-plagioclase gneiss (sample XX43-2); (b) metapelite (sample SN14-1).

strong mylonitization of the most rocks. Quartz forms obviously elongated ribbon or occurs as polycrystalline aggregates. The bands of sericite + chlorite + epidote are commonly developed. Plagioclase grains are mostly subjected to saussuritization and sericitization.

Metapelite sample SN14-1 was collected from a layer of ~30 m thick (Figure 2(b)), and the country rocks are fine-grained banded granitic gneiss. It is mainly composed of garnet (20%), biotite (25%), plagioclase (20%) and quartz (30%), with minor sillimanite, kyanite, staurolite, rutile and ilmenite (5%). The rock shows porphyritic texture, with euhedral garnet porphyroblasts up to 3–25 mm. Garnet contains inclusions of biotite, kyanite, rutile, quartz and ilmenite. Secondary chlorites occasionally occur in the garnet rim. Biotite together with fibrolitic sillimanite commonly develops around garnet porphyroblasts. Quartz often displays as banded aggregations, in which garnet sometimes is enriched.

2.2 Analytical procedures

Zircon crystals were extracted from samples of several kilograms using the conventional techniques, including crushing, sieving, heavy liquid and hand picking. Zircon grains were mounted on epoxy disc and polished down to their two-thirds exposed. The internal structures of zircons were revealed by cathodoluminescence (CL) imaging. The zircon analyses were performed using laser ablation multi-collector inductively coupled plasma mass spectrometry (LA-MC-ICP-MS) at the Tianjin Institute of Geology and Mineral Resources. A detailed compilation of instrumental conditions was given by Li et al. [31]. The spot diameters were set to be 35 μm with laser frequency at 8–10 Hz for all samples, and the density of plasma was 13–14 J/cm^3. TEMORA zircon standard was used as an external standard for U-Pb dating. Data processing was completed using ICPMSDataCal [32,33] and ISOPLOT [34]. The conventional ^{208}Pb correction was performed. NIST612 was analyzed twice after every six analyses to determine the concentrations of Pb, U and Th. The age uncertainty for individual analysis represents one standard deviation (1σ), but the calculated weighted mean ages are quoted at the 95% confidence level. The analytical data are listed in Table 2.

Zircon Hf isotopic analyses were conducted *in-situ* using

Table 2 LA-MC-ICPMS U-Pb analyses of zircons for dioritic-granitic gneisses and metasedimentary rock from the Douling Complex

Spot	U (ppm)	Th (ppm)	Th/U	Isotopic ratios						Age (Ma)						Degree of concordance (%)
				^{207}Pb/^{206}Pb	±σ	^{207}Pb/^{235}U	±σ	^{206}Pb/^{238}U	±σ	^{207}Pb/^{206}Pb	±σ	^{207}Pb/^{235}U	±σ	^{206}Pb^{238}U	±σ	
Sample XX09-1 (amphibole-plagioclase gneiss)																
Oscillatory core																
1	209	15	0.07	0.1177	0.0016	3.826	0.076	0.2359	0.0024	1921	25	1598	32	1365	14	71
2	135	3.5	0.03	0.0707	0.0014	1.429	0.029	0.1466	0.0014	948	39	901	18	882	9	93
3	31	19	0.60	0.1645	0.0029	10.567	0.184	0.4660	0.0043	2502	29	2486	43	2466	23	99
4	147	47	0.32	0.1381	0.0018	6.191	0.101	0.3251	0.0026	2204	22	2003	33	1815	14	82
5	274	73	0.27	0.1430	0.0017	6.794	0.089	0.3446	0.0031	2264	21	2085	27	1909	17	84
6	199	111	0.56	0.1495	0.0018	8.877	0.132	0.4308	0.0030	2340	21	2325	35	2309	16	99
7	45	25	0.55	0.1618	0.0023	10.264	0.150	0.4601	0.0042	2474	24	2459	36	2440	23	99
8	73	66	0.90	0.1509	0.0020	8.207	0.120	0.3944	0.0039	2356	22	2254	33	2143	21	91
9	665	86	0.13	0.1433	0.0017	6.843	0.084	0.3463	0.0031	2267	20	2091	26	1917	17	85
10	367	58	0.16	0.0983	0.0013	2.621	0.040	0.1934	0.0018	1592	24	1306	20	1140	11	72
11	176	12	0.07	0.0912	0.0015	2.265	0.046	0.1800	0.0017	1451	32	1201	24	1067	10	74
12	278	64	0.23	0.1566	0.0019	9.272	0.114	0.4295	0.0040	2419	20	2365	29	2304	22	95
13	49	4	0.09	0.0910	0.0037	2.220	0.089	0.1770	0.0024	1446	77	1187	48	1050	14	73
14	205	51	0.25	0.1393	0.0019	5.999	0.125	0.3124	0.0035	2218	24	1976	41	1752	20	79
15	335	191	0.57	0.1471	0.0018	7.243	0.094	0.3570	0.0036	2313	21	2142	28	1968	20	85
16	710	50	0.07	0.1421	0.0017	6.557	0.080	0.3347	0.0029	2253	20	2054	25	1861	16	83
17	145	42	0.29	0.0714	0.0012	1.602	0.029	0.1627	0.0014	969	36	971	17	972	8	100
18	285	60	0.21	0.1038	0.0013	3.044	0.040	0.2126	0.0019	1694	24	1419	19	1243	11	73
Grey overgrowth																
19	306	132	0.43	0.1027	0.0013	3.446	0.055	0.2434	0.0019	1673	23	1515	24	1404	11	84
20	362	7	0.02	0.0697	0.0010	1.333	0.020	0.1388	0.0014	918	29	860	13	838	8	91
21	301	27	0.09	0.1160	0.0014	3.356	0.048	0.2097	0.0019	1896	22	1494	22	1227	11	65
22	84	0.3	0.00	0.0696	0.0028	1.333	0.056	0.1390	0.0013	916	84	860	36	839	8	92
23	71	0.3	0.00	0.0697	0.0035	1.320	0.068	0.1374	0.0013	918	104	854	44	830	8	90
24	208	1	0.01	0.0681	0.0011	1.308	0.022	0.1392	0.0013	873	34	849	14	840	8	96
SampleXX43-2 (amphibole-plagioclase gneiss)																
1	61	75	1.23	0.1615	0.0017	10.489	0.131	0.4709	0.0057	2472	17	2479	31	2487	30	101

(*To be continued on the next page*)

(*Continued*)

Spot	U (ppm)	Th (ppm)	Th/U	Isotopic ratios						Age (Ma)						Degree of concordance (%)
				$^{207}Pb/^{206}Pb$	±σ	$^{207}Pb/^{235}U$	±σ	$^{206}Pb/^{238}U$	±σ	$^{207}Pb/^{206}Pb$	±σ	$^{207}Pb/^{235}U$	±σ	$^{206}Pb^{238}U$	±σ	
2	28	34	1.22	0.1612	0.0029	10.430	0.202	0.4693	0.0041	2468	31	2474	48	2481	22	100
3	51	77	1.50	0.1614	0.0018	10.398	0.123	0.4674	0.0043	2470	19	2471	29	2472	23	100
4	67	59	0.88	0.1611	0.0017	10.349	0.127	0.4659	0.0038	2467	18	2467	30	2466	20	100
5	46	68	1.48	0.1594	0.0021	10.001	0.269	0.4549	0.0045	2450	22	2435	65	2417	24	99
6	105	112	1.07	0.1594	0.0015	9.405	0.097	0.4279	0.0045	2449	16	2378	25	2296	24	94
7	62	67	1.09	0.1625	0.0018	10.408	0.126	0.4645	0.0038	2482	19	2472	30	2459	20	99
8	82	82	1.01	0.1616	0.0017	10.438	0.117	0.4685	0.0041	2472	18	2474	28	2477	22	100
9	82	105	1.28	0.1540	0.0019	8.590	0.122	0.4045	0.0036	2391	21	2295	33	2190	20	92
10	101	100	0.99	0.1614	0.0015	9.957	0.103	0.4474	0.0039	2471	16	2431	25	2384	21	96
11	37	62	1.66	0.1615	0.0021	10.434	0.155	0.4685	0.0042	2472	22	2474	37	2477	22	100
12	61	56	0.92	0.1588	0.0030	10.050	0.199	0.4591	0.0044	2443	32	2439	48	2435	23	100
13	28	46	1.66	0.1601	0.0024	10.322	0.161	0.4676	0.0048	2457	25	2464	38	2473	26	101
14	38	55	1.45	0.1604	0.0021	10.181	0.145	0.4604	0.0040	2460	23	2451	35	2441	21	99
15	36	67	1.88	0.1630	0.0025	10.410	0.171	0.4633	0.0049	2487	26	2472	41	2454	26	99
16	69	58	0.84	0.1618	0.0016	10.367	0.139	0.4646	0.0068	2475	17	2468	33	2460	36	99
17	266	156	0.59	0.1632	0.0015	9.575	0.123	0.4255	0.0057	2489	16	2395	31	2285	30	92
18	36	53	1.45	0.1626	0.0021	10.522	0.156	0.4694	0.0054	2482	22	2482	37	2481	29	100
19	119	84	0.71	0.1639	0.0013	10.530	0.098	0.4661	0.0038	2496	13	2483	23	2466	20	99
20	89	92	1.04	0.1602	0.0013	9.933	0.099	0.4498	0.0041	2457	14	2429	24	2394	22	97
21	30	39	1.29	0.1635	0.0030	10.521	0.197	0.4667	0.0058	2492	31	2482	46	2469	31	99
22	28	50	1.78	0.1627	0.0028	10.582	0.194	0.4716	0.0049	2484	29	2487	46	2491	26	100
23	45	67	1.47	0.1616	0.0020	10.141	0.134	0.4553	0.0039	2472	21	2448	32	2419	21	98
24	61	58	0.95	0.1612	0.0019	10.370	0.139	0.4665	0.0036	2468	20	2468	33	2468	19	100
Sample XP08-4 (plagioclase gneiss)																
1	103	117	1.14	0.1621	0.0021	9.967	0.131	0.4463	0.0035	2477	22	2432	32	2379	19	96
2	111	75	0.68	0.1623	0.0022	9.152	0.128	0.4091	0.0031	2480	23	2353	33	2211	17	89
3	50	39	0.78	0.1629	0.0024	10.202	0.156	0.4543	0.0035	2486	25	2453	37	2414	19	97
4	47	52	1.11	0.1638	0.0024	10.160	0.150	0.4501	0.0037	2495	24	2449	36	2396	20	96
5	71	66	0.93	0.1632	0.0021	10.295	0.138	0.4575	0.0037	2490	22	2462	33	2429	19	98
6	106	235	1.25	0.1634	0.0021	10.184	0.132	0.4521	0.0032	2491	21	2452	32	2405	17	97
7	124	133	1.20	0.1621	0.0020	9.886	0.127	0.4425	0.0031	2477	21	2424	31	2362	17	95
8	113	87	0.77	0.1634	0.0021	8.552	0.112	0.3800	0.0036	2491	22	2291	30	2076	19	83
9	52	33	0.63	0.1645	0.0024	8.724	0.134	0.3845	0.0033	2503	25	2310	35	2097	18	84
10	59	31	0.52	0.1630	0.0030	7.492	0.145	0.3331	0.0033	2487	31	2172	42	1854	18	75
11	44	77	1.74	0.1607	0.0023	9.554	0.144	0.4311	0.0034	2463	25	2393	36	2311	18	94
12	52	40	0.76	0.1645	0.0022	9.632	0.134	0.4245	0.0033	2503	23	2400	33	2281	18	91
13	97	79	0.81	0.1628	0.0021	9.379	0.123	0.4179	0.0032	2485	21	2376	31	2251	17	91
14	64	55	0.86	0.1575	0.0023	8.549	0.130	0.3937	0.0031	2429	25	2291	35	2140	17	88
15	59	38	0.64	0.1558	0.0022	8.765	0.127	0.4082	0.0033	2410	24	2314	34	2207	18	92
16	279	36	0.13	0.1555	0.0020	8.312	0.118	0.3876	0.0062	2407	21	2266	32	2112	34	88
17	103	90	0.87	0.1610	0.0020	9.972	0.130	0.4494	0.0032	2466	21	2432	32	2392	17	97
18	48	94	1.95	0.1640	0.0022	10.321	0.142	0.4566	0.0039	2497	23	2464	34	2424	20	97
19	75	56	0.74	0.1620	0.0021	9.926	0.134	0.4443	0.0032	2477	22	2428	33	2370	17	96
20	66	50	0.75	0.1638	0.0022	10.544	0.142	0.4670	0.0039	2495	22	2484	33	2471	21	99
21	75	44	0.59	0.1644	0.0022	9.580	0.128	0.4227	0.0031	2501	22	2395	32	2273	16	91
22	49	275	5.61	0.1655	0.0025	10.292	0.159	0.4513	0.0035	2512	26	2461	38	2401	19	96
23	76	46	0.60	0.1513	0.0022	7.652	0.114	0.3669	0.0031	2360	25	2191	33	2015	17	85
24	89	80	0.90	0.1632	0.0021	10.434	0.139	0.4636	0.0032	2490	22	2474	33	2456	17	99
Sample XP16-4 (two-feldspar gneiss)																
1	429	236	0.55	0.1593	0.0022	9.604	0.138	0.4374	0.0037	2448	23	2398	34	2339	20	96
2	569	296	0.52	0.1624	0.0022	10.213	0.147	0.4561	0..0042	2481	23	2454	35	2422	23	98
3	529	217	0.41	0.1617	0.0022	10.323	0.148	0.4631	0.0037	2473	23	2464	35	2453	20	99
4	899	90	0.10	0.1593	0.0022	9.871	0.144	0.4494	0.0053	2448	23	2423	35	2392	28	98
5	346	104	0.30	0.1633	0.0022	9.381	0.134	0.4166	0.0032	2490	23	2376	34	2245	17	90
6	389	179	0.46	0.1622	0.0022	10.302	0.148	0.4607	0.0042	2479	23	2462	35	2443	22	99

(*To be continued on the next page*)

(*Continued*)

Spot	U (ppm)	Th (ppm)	Th/U	Isotopic ratios						Age (Ma)						Degree of concordance (%)
				$^{207}Pb/^{206}Pb$	±σ	$^{207}Pb/^{235}U$	±σ	$^{206}Pb/^{238}U$	±σ	$^{207}Pb/^{206}Pb$	±σ	$^{207}Pb/^{235}U$	±σ	$^{206}Pb^{238}U$	±σ	
7	385	123	0.32	0.1698	0.0024	10.595	0.156	0.4526	0.0034	2556	23	2488	37	2407	18	94
8	418	113	0.27	0.1625	0.0022	10.674	0.153	0.4764	0.0043	2482	23	2495	36	2512	22	101
9	393	157	0.40	0.1609	0.0022	10.039	0.144	0.4525	0.0035	2465	23	2438	35	2406	19	98
10	409	213	0.52	0.1636	0.0022	10.660	0.152	0.4726	0.0036	2493	23	2494	36	2495	19	100
11	462	217	0.47	0.1631	0.0022	10.775	0.155	0.4790	0.0045	2489	23	2504	36	2523	24	101
12	319	112	0.35	0.1635	0.0022	10.536	0.151	0.4672	0.0043	2493	23	2483	36	2471	23	99
13	1453	247	0.17	0.1331	0.0018	4.305	0.062	0.2345	0.0018	2140	24	1694	24	1358	10	63
14	488	137	0.28	0.1660	0.0023	10.942	0.157	0.4782	0.0037	2517	23	2518	36	2520	20	100
15	1452	131	0.09	0.1585	0.0022	9.762	0.141	0.4466	0.0044	2440	23	2413	35	2380	23	98
16	507	188	0.37	0.1649	0.0023	11.061	0.158	0.4865	0.0044	2507	23	2528	36	2555	23	102
17	1511	196	0.13	0.1649	0.0022	10.741	0.154	0.4724	0.0041	2507	23	2501	36	2494	21	99
18	649	123	0.19	0.1636	0.0022	10.347	0.148	0.4586	0.0039	2494	23	2466	35	2433	21	98
19	369	162	0.44	0.1693	0.0023	10.621	0.152	0.4550	0.0036	2551	23	2491	36	2417	19	95
20	593	213	0.36	0.1640	0.0022	9.850	0.141	0.4357	0.0034	2497	23	2421	35	2331	18	93
21	980	176	0.18	0.0627	0.0022	10.558	0.151	0.4707	0.0043	2484	23	2484	36	2486	23	100
22	615	172	0.28	0.1690	0.0023	11.249	0.163	0.4828	0.0049	2548	23	2544	37	2539	26	100
23	326	130	0.40	0.1826	0.0025	12.677	0.182	0.5035	0.0043	2677	23	2656	38	2629	23	98
24	607	170	0.28	0.1585	0.0022	9.918	0.144	0.4538	0.0052	2440	23	2427	35	2412	28	99
Sample SN07-7 (biotite-plagioclase gneiss)																
Oscillatory core																
1	864	138	0.16	0.1643	0.0020	9.204	0.146	0.4063	0.0032	2500	21	2358	37	2198	18	88
2	468	84	0.18	0.1625	0.0020	8.769	0.113	0.3913	0.0033	2482	21	2314	30	2129	18	86
3	1122	247	0.22	0.1650	0.0020	10.474	0.154	0.4604	0.0081	2507	21	2512	37	2442	43	97
4	695	91	0.13	0.1660	0.0021	10.295	0.170	0.4499	0.0061	2517	21	2462	41	2395	32	95
5	655	144	0.22	0.1631	0.0020	9.561	0.138	0.4251	0.0084	2488	21	2393	34	2284	45	92
6	254	94	0.37	0.1737	0.0022	11.818	0.152	0.4935	0.0042	2594	21	2590	33	2586	22	100
7	586	182	0.31	0.1765	0.0022	12.301	0.158	0.5054	0.0041	2621	21	2628	34	2637	22	101
8	617	80	0.13	0.1734	0.0021	11.085	0.144	0.4636	0.0047	2591	21	2530	33	2455	25	95
9	1094	164	0.15	0.1482	0.0018	4.514	0.062	0.2209	0.0041	2326	21	1734	24	1286	24	55
10	417	96	0.23	0.1745	0.0022	11.716	0.153	0.4871	0.0050	2601	21	2582	34	2558	27	98
11	878	167	0.19	0.1691	0.0021	9.195	0.118	0.3943	0.0035	2549	21	2358	30	2143	19	84
12	184	118	0.64	0.1638	0.0020	10.539	0.137	0.4666	0.0041	2495	21	2483	32	2469	22	99
13	456	91	0.20	0.1732	0.0021	10.493	0.135	0.4395	0.0037	2588	21	2505	32	2348	20	91
14	475	143	0.30	0.1773	0.0022	12.105	0.155	0.4951	0.0043	2628	21	2613	33	2593	23	99
15	482	164	0.34	0.1763	0.0022	12.147	0.156	0.4997	0.0041	2618	21	2639	34	2612	21	100
16	165	152	0.92	0.1638	0.0020	10.543	0.163	0.4667	0.0038	2496	21	2484	32	2469	20	99
17	762	267	0.35	0.1766	0.0022	11.992	0.153	0.4926	0.0040	2621	21	2604	33	2582	21	99
18	370	152	0.41	0.1692	0.0021	11.118	0.144	0.4765	0.0044	2550	21	2533	33	2512	23	99
19	599	162	0.27	0.1776	0.0022	11.387	0.146	0.4651	0.0039	2630	21	2555	33	2462	20	94
20	302	130	0.43	0.1830	0.0023	13.073	0.168	0.5180	0.0045	2681	21	2685	35	2691	24	100
21	914	292	0.32	0.1594	0.0020	7.807	0.115	0.3553	0.0033	2449	21	2209	32	1960	18	80
22	377	128	0.34	0.1761	0.0022	11.841	0.152	0.4878	0.0042	2616	21	2592	33	2561	22	98
23	562	112	0.20	0.1764	0.0022	12.112	0.161	0.4979	0.0067	2620	21	2613	35	2605	35	99
24	567	153	0.27	0.1741	0.0022	11.728	0.150	0.4884	0.0040	2598	21	2583	33	2564	21	99
Grey mantle																
25	208	83	0.40	0.1604	0.0020	10.150	0.132	0.4590	0.0046	2460	21	2448	32	2435	24	99
26	65	24	0.38	0.1306	0.0022	4.446	0.078	0.2469	0.0045	2106	29	1721	30	1422	26	68
27	238	90	0.38	0.1781	0.0022	11.478	0.152	0.4674	0.0051	2635	21	2563	34	2472	27	94
28	130	164	1.26	0.1590	0.0020	9.972	0.130	0.4549	0.0039	2445	21	2432	32	2417	21	99
29	121	136	1.12	0.1648	0.0021	10.031	0.132	0.4415	0.0040	2505	22	2438	32	2357	21	94
30	199	80	0.40	0.1575	0.0020	9.160	0.119	0.4218	0.0042	2429	21	2354	30	2269	22	93
Sample SN14-1 (metapelite)																
1	87	49	0.56	0.0894	0.0017	2.884	0.062	0.2339	0.0044	1413	37	1378	30	1355	26	96
2	135	69	0.51	0.1699	0.0016	11.134	0.138	0.4752	0.0067	2557	15	2534	31	2506	35	98
3	158	78	0.50	0.1783	0.0015	12.218	0.126	0.4969	0.0058	2637	14	2621	27	2601	31	99

(*To be continued on the next page*)

(*Continued*)

Spot	U (ppm)	Th (ppm)	Th/U	Isotopic ratios						Age (Ma)						Degree of concordance (%)
				$^{207}Pb/^{206}Pb$	$\pm\sigma$	$^{207}Pb/^{235}U$	$\pm\sigma$	$^{206}Pb/^{238}U$	$\pm\sigma$	$^{207}Pb/^{206}Pb$	$\pm\sigma$	$^{207}Pb/^{235}U$	$\pm\sigma$	$^{206}Pb^{238}U$	$\pm\sigma$	
4	121	58	0.48	0.1819	0.0015	12.325	0.137	0.4915	0.0064	2670	14	2629	29	2577	34	97
5	366	146	0.40	0.1871	0.0016	10.607	0.107	0.4110	0.0035	2717	14	2489	25	2220	19	82
6	113	77	0.68	0.1657	0.0016	10.754	0.122	0.4708	0.0044	2514	16	2502	28	2487	23	99
7	116	75	0.65	0.1325	0.0015	6.761	0.095	0.3700	0.0044	2132	20	2081	29	2030	24	95
8	53	55	1.05	0.1251	0.0021	6.152	0.118	0.3566	0.0044	2031	30	1998	38	1966	24	97
9	229	72	0.32	0.1577	0.0019	7.483	0.108	0.3442	0.0035	2431	20	2171	31	1907	20	78
10	829	9	0.01	0.0966	0.0010	2.746	0.041	0.2061	0.0031	1560	19	1341	20	1208	18	77
11	271	204	0.75	0.0878	0.0010	2.887	0.039	0.2384	0.0028	1379	21	1379	19	1378	16	100
12	163	72	0.44	0.1775	0.0017	11.622	0.143	0.4749	0.0063	2630	16	2574	32	2505	33	95
13	159	104	0.65	0.1940	0.0019	14.011	0.193	0.5238	0.0082	2776	16	2750	38	2715	42	98
14	240	94	0.39	0.1781	0.0018	11.486	0.152	0.4677	0.0059	2635	17	2563	34	2473	31	94
15	194	189	0.98	0.1601	0.0018	9.627	0.129	0.4362	0.0049	2457	19	2400	32	2333	26	95
16	185	2	0.01	0.0676	0.0015	1.246	0.030	0.1337	0.0019	857	45	822	20	809	11	94
17	182	4	0.02	0.0657	0.0015	1.213	0.030	0.1340	0.0016	797	48	807	20	810	10	102
18	152	102	0.67	0.1230	0.0014	6.068	0.081	0.3579	0.0041	2000	21	1986	27	1972	23	99
19	333	178	0.54	0.1686	0.0017	9.328	0.122	0.4014	0.0057	2543	17	2371	31	2175	31	86
20	395	96	0.24	0.1402	0.0014	6.405	0.078	0.3314	0.0033	2230	17	2033	25	1845	19	83
21	166	99	0.60	0.1600	0.0015	9.983	0.113	0.4524	0.0041	2456	16	2433	28	2406	22	98
22	325	228	0.70	0.1769	0.0017	11.168	0.135	0.4579	0.0053	2624	16	2537	31	2430	28	93
23	371	120	0.32	0.1480	0.0015	7.155	0.096	0.3506	0.0047	2323	18	2131	29	1938	26	83
24	113	70	0.62	0.0932	0.0014	3.479	0.059	0.2708	0.0036	1492	28	1523	26	1545	21	104
25	240	75	0.31	0.1608	0.0018	10.012	0.121	0.4515	0.0039	2464	19	2436	29	2402	21	97
26	310	149	0.48	0.1770	0.0018	11.017	0.209	0.4513	0.0102	2625	17	2525	48	2401	54	91
27	32	21	0.65	0.1303	0.0025	6.884	0.141	0.3832	0.0041	2102	34	2097	43	2091	22	100
28	538	123	0.23	0.1488	0.0013	7.480	0.075	0.3645	0.0030	2332	15	2171	22	2003	17	86
29	111	72	0.65	0.1624	0.0015	10.215	0.112	0.4562	0.0046	2481	16	2454	27	2423	24	98
30	220	49	0.22	0.1732	0.0017	10.172	0.107	0.4259	0.0030	2589	16	2451	26	2287	16	88
31	356	187	0.53	0.0885	0.0010	2.889	0.034	0.2368	0.0020	1393	21	1379	16	1370	12	98
32	116	68	0.59	0.0888	0.0015	2.899	0.052	0.2367	0.0021	1401	32	1382	25	1369	12	98
33	226	225	0.99	0.1755	0.0020	11.193	0.168	0.4626	0.0068	2611	19	2539	38	2451	36	94
34	10	0.3	0.03	0.1212	0.0146	5.910	0.730	0.3537	0.0118	1973	215	1963	242	1952	65	99
35	63	32	0.51	0.0908	0.0024	2.935	0.079	0.2345	0.0026	1442	51	1391	38	1358	15	94
36	326	75	0.23	0.1769	0.0016	8.398	0.094	0.3444	0.0044	2624	15	2275	25	1908	24	73
37	195	117	0.60	0.0870	0.0010	2.861	0.036	0.2383	0.0021	1362	23	1372	17	1378	12	101
38	103	62	0.60	0.1929	0.0018	13.873	0.148	0.5215	0.0046	2767	16	2741	29	2706	24	98
39	168	41	0.25	0.1635	0.0016	10.204	0.111	0.4526	0.0038	2493	17	2453	27	2407	20	97
40	210	2	0.01	0.0668	0.0014	1.260	0.026	0.1368	0.0013	831	43	828	17	827	8	100
41	159	109	0.69	0.1709	0.0019	11.089	0.147	0.4706	0.0064	2566	18	2531	34	2486	34	97
42	107	69	0.64	0.1604	0.0017	10.212	0.122	0.4619	0.0050	2459	18	2454	29	2448	26	100
43	317	102	0.32	0.1209	0.0011	5.825	0.060	0.3494	0.0032	1970	16	1950	20	1932	17	98
44	224	83	0.37	0.1652	0.0014	10.555	0.104	0.4634	0.0045	2510	15	2485	25	2455	24	98
45	76	39	0.51	0.1621	0.0017	10.230	0.120	0.4576	0.0042	2478	18	2456	29	2429	22	98
46	121	54	0.45	0.1682	0.0017	9.516	0.109	0.4103	0.0036	2540	16	2389	27	2216	20	87
47	52	51	0.97	0.1309	0.0019	6.651	0.130	0.3685	0.0072	2110	25	2066	40	2022	40	96
48	133	1	0.01	0.0654	0.0015	1.224	0.029	0.1357	0.0018	788	48	812	19	820	11	104
49	302	63	0.21	0.1710	0.0018	10.518	0.135	0.4461	0.0061	2567	18	2481	32	2378	32	93
50	140	26	0.19	0.1720	0.0017	11.203	0.138	0.4724	0.0059	2577	17	2540	31	2494	31	97
51	374	236	0.63	0.1753	0.0016	11.184	0.132	0.4627	0.0063	2609	15	2539	30	2451	34	94
52	169	3	0.02	0.1200	0.0012	5.616	0.064	0.3394	0.0035	1956	18	1919	22	1884	20	96
53	166	93	0.56	0.1818	0.0016	12.493	0.148	0.4985	0.0067	2669	15	2642	31	2607	35	98
54	378	158	0.42	0.1523	0.0014	8.147	0.095	0.3879	0.0048	2372	16	2247	26	2113	26	89
55	28	1	0.04	0.1208	0.0041	5.756	0.203	0.3454	0.0039	1969	60	1940	68	1913	21	97
56	67	30	0.45	0.1769	0.0023	10.936	0.163	0.4483	0.0058	2624	21	2518	38	2388	31	91
57	201	88	0.44	0.1759	0.0020	11.541	0.168	0.4759	0.0079	2614	19	2568	37	2509	42	96
58	13	0.1	0.01	0.1151	0.0128	5.735	0.649	0.3613	0.0086	1882	200	1937	219	1988	47	106
59	101	94	0.94	0.1231	0.0015	5.956	0.083	0.3508	0.0038	2002	22	1969	27	1939	21	97
60	189	128	0.68	0.1631	0.0016	10.071	0.116	0.4477	0.0044	2488	16	2441	28	2385	24	96

(*To be continued on the next page*)

(*Continued*)

Spot	U (ppm)	Th (ppm)	Th/U	Isotopic ratios						Age (Ma)						Degree of concordance (%)
				$^{207}Pb/^{206}Pb$	$\pm\sigma$	$^{207}Pb/^{235}U$	$\pm\sigma$	$^{206}Pb/^{238}U$	$\pm\sigma$	$^{207}Pb/^{206}Pb$	$\pm\sigma$	$^{207}Pb/^{235}U$	$\pm\sigma$	$^{206}Pb^{238}U$	$\pm\sigma$	
62	75	28	0.37	0.1786	0.0021	12.036	0.198	0.4889	0.0086	2640	20	2607	43	2566	45	97
63	47	26	0.56	0.1191	0.0023	5.735	0.136	0.3491	0.0070	1943	35	1937	46	1930	39	99
64	70	32	0.46	0.1671	0.0023	10.340	0.175	0.4487	0.0069	2529	24	2466	42	2389	37	94
65	403	201	0.50	0.1686	0.0022	9.275	0.142	0.3990	0.0059	2544	22	2366	36	2165	32	85
66	454	154	0.34	0.1574	0.0018	7.308	0.095	0.3367	0.0032	2428	20	2150	28	1871	18	77
67	277	108	0.39	0.1791	0.0019	10.981	0.133	0.4447	0.0044	2644	18	2522	31	2372	23	90
68	145	42	0.29	0.1781	0.0018	11.608	0.147	0.4727	0.0063	2635	17	2573	32	2495	33	95
69	107	21	0.19	0.1657	0.0018	10.439	0.148	0.4569	0.0056	2515	18	2475	35	2426	30	96
70	395	222	0.56	0.1696	0.0018	8.679	0.098	0.3711	0.0029	2554	17	2305	26	2035	16	80
71	419	227	0.54	0.1607	0.0018	7.530	0.093	0.3398	0.0029	2463	19	2177	27	1886	16	77
72	254	49	0.19	0.1651	0.0021	9.194	0.208	0.4038	0.0110	2509	21	2358	53	2187	60	87
73	96	47	0.49	0.1710	0.0023	10.324	0.187	0.4378	0.0075	2568	22	2464	45	2341	40	91
74	181	108	0.59	0.1718	0.0019	10.721	0.145	0.4527	0.0057	2575	19	2499	34	2407	30	93
75	135	107	0.79	0.0895	0.0014	2.891	0.053	0.2344	0.0032	1414	29	1380	25	1357	19	96
76	61	24	0.40	0.1762	0.0019	10.923	0.145	0.4497	0.0056	2617	18	2517	33	2394	30	91
77	51	23	0.46	0.0878	0.0024	2.827	0.082	0.2335	0.0029	1378	52	1363	39	1353	17	98
78	73	42	0.57	0.1778	0.0021	11.995	0.153	0.4894	0.0043	2632	19	2604	33	2568	23	98
79	452	133	0.29	0.1419	0.0015	6.339	0.101	0.3239	0.0054	2251	19	2024	32	1809	30	80
80	322	15	0.05	0.1425	0.0017	7.329	0.095	0.3731	0.0035	2257	21	2152	28	2044	19	91
81	83	42	0.50	0.1550	0.0020	8.736	0.129	0.4087	0.0053	2402	22	2311	34	2209	29	92
82	341	61	0.18	0.1421	0.0016	5.317	0.068	0.2714	0.0025	2253	19	1872	24	1548	14	69
83	294	87	0.30	0.1716	0.0017	10.273	0.124	0.4343	0.0049	2573	17	2460	30	2325	26	90
84	108	70	0.65	0.1732	0.0017	11.376	0.125	0.4764	0.0044	2589	16	2554	28	2512	23	97
85	121	56	0.46	0.1639	0.0016	9.350	0.100	0.4138	0.0034	2496	16	2373	25	2232	18	89
86	99	40	0.41	0.1502	0.0016	8.407	0.118	0.4060	0.0057	2348	18	2276	32	2197	31	94
87	105	75	0.72	0.1256	0.0015	6.337	0.105	0.3658	0.0066	2038	21	2024	34	2010	36	99
88	189	88	0.46	0.1642	0.0019	9.612	0.149	0.4246	0.0071	2499	19	2398	37	2281	38	91
89	268	113	0.42	0.1549	0.0017	9.020	0.112	0.4224	0.0046	2400	19	2340	29	2271	25	95
90	215	87	0.40	0.1729	0.0018	10.616	0.120	0.4454	0.0041	2586	17	2490	28	2375	22	92
91	287	177	0.62	0.1638	0.0017	8.681	0.148	0.3845	0.0072	2495	17	2305	39	2097	39	84
92	49	14	0.29	0.1535	0.0019	8.534	0.124	0.4033	0.0046	2385	21	2290	33	2184	25	92
93	135	145	1.08	0.1187	0.0013	5.365	0.073	0.3277	0.0042	1937	19	1879	26	1827	23	94
94	526	49	0.09	0.1701	0.0017	10.234	0.167	0.4364	0.0086	2558	17	2456	40	2335	46	91
95	174	119	0.68	0.1259	0.0014	6.379	0.087	0.3675	0.0044	2041	20	2029	28	2018	24	99
96	298	191	0.64	0.1762	0.0021	11.322	0.159	0.4660	0.0054	2617	20	2550	36	2466	29	94
97	181	61	0.34	0.1720	0.0021	10.993	0.148	0.4634	0.0045	2578	20	2523	34	2455	24	95
98	131	14	0.10	0.1733	0.0019	11.070	0.170	0.4633	0.0077	2590	18	2529	39	2454	41	95
99	50	41	0.82	0.1408	0.0022	6.731	0.108	0.3466	0.0033	2237	27	2077	33	1918	18	86
100	173	62	0.36	0.1615	0.0015	9.506	0.111	0.4268	0.0045	2472	16	2388	28	2291	24	93
101	102	27	0.27	0.1298	0.0015	6.476	0.083	0.3618	0.0030	2096	20	2043	26	1990	17	95
102	206	23	0.11	0.1657	0.0017	9.532	0.164	0.4173	0.0088	2514	17	2391	41	2248	47	89
103	257	116	0.45	0.1522	0.0016	7.647	0.097	0.3644	0.0039	2371	18	2190	28	2003	22	84
104	265	65	0.24	0.1692	0.0020	10.174	0.136	0.4361	0.0046	2550	19	2451	33	2333	25	92
105	207	80	0.39	0.1395	0.0017	7.336	0.114	0.3815	0.0047	2221	21	2153	33	2083	26	94
106	139	18	0.13	0.1746	0.0019	11.365	0.157	0.4721	0.0059	2602	18	2554	35	2493	31	96
107	140	67	0.48	0.1844	0.0019	12.355	0.146	0.4860	0.0048	2693	17	2632	31	2553	25	95
108	315	89	0.28	0.1709	0.0016	10.336	0.128	0.4385	0.0054	2567	15	2465	30	2344	29	91
109	312	149	0.48	0.1622	0.0015	9.650	0.137	0.4314	0.0068	2479	16	2402	34	2312	36	93
110	789	71	0.09	0.1066	0.0011	3.449	0.041	0.2346	0.0025	1742	18	1516	18	1359	15	78
111	154	43	0.28	0.1830	0.0020	12.426	0.141	0.4923	0.0041	2681	18	2637	30	2581	22	96
112	213	143	0.67	0.1793	0.0021	11.910	0.156	0.4817	0.0049	2647	19	2597	34	2535	26	96
113	196	66	0.34	0.2272	0.0026	17.901	0.224	0.5715	0.0051	3032	19	2984	37	2914	26	96
114	126	30	0.24	0.2010	0.0022	13.084	0.169	0.4722	0.0055	2834	18	2686	35	2493	29	88
115	399	59	0.15	0.1677	0.0016	10.413	0.132	0.4503	0.0057	2535	16	2472	31	2396	30	95
116	176	90	0.51	0.1606	0.0016	9.773	0.108	0.4412	0.0038	2462	16	2414	27	2356	20	96
117	163	74	0.45	0.1635	0.0016	10.162	0.106	0.4508	0.0033	2492	16	2450	26	2399	18	96
118	505	182	0.36	0.1610	0.0017	7.993	0.106	0.3600	0.0039	2467	18	2230	30	1982	22	80
119	221	110	0.50	0.1803	0.0020	11.958	0.136	0.4810	0.0038	2656	18	2601	30	2532	20	95
120	357	181	0.51	0.1735	0.0021	11.076	0.142	0.4630	0.0045	2592	20	2530	32	2453	24	95

a Neptune MC-ICP-MS with a New Wave UP213 laser ablation system at the Institute of Mineral Resources, Chinese Academy of Geological Sciences, Beijing. The analyses were performed on the same or nearby zircon domains on which the U-Pb dating had been conducted. All analyses were performed with a beam diameter of 40 μm. Helium was used as a carrier gas to provide efficient aerosol delivered to the torch. The instrumental conditions and data acquisition have been comprehensively described by Hou et al. [32] Zircon GJ1 was used as the reference standard during our routine analyses, with a weighted mean $^{176}Hf/^{177}Hf$ ratio of 0.281996 ± 1 (2SD, n = 12), which is in good agreement with the previously reported data within errors [35,36]. We chose two-stage Hf model age (T_{Hf2}) for tracing material source [37]. The analytical results are presented in Table 3.

3 Geochronological results

3.1 Amphibole-plagioclase gneiss (sample XX09-1)

The zircons from the amphibole-plagioclase gneiss sample XX09-1 are prismatic to rounded in shape, with 60–260 μm

Table 3 LA-MC-ICPMS Hf isotopic analyses of zircons for dioritic-granitic gneisses from the Douling Complex

Spot	t (Ma)	$^{176}Yb/^{177}Hf$	$^{176}Lu/^{177}Hf$	$^{176}Hf/^{177}Hf$	2σ	$\varepsilon_{Hf}(0)$	2σ	$\varepsilon_{Hf}(t)$	2σ	T_{Hf1}	T_{Hf2}	2σ	$f_{Lu/Hf}$
Sample XX43-2 (amphibole-plagioclase gneiss)													
1	2472	0.021970	0.000377	0.281051	0.000026	−60.8	0.9	−6.1	0.9	3011	3345	67	−0.99
2	2468	0.014839	0.000252	0.281052	0.000024	−60.8	0.9	−5.9	0.9	3000	3333	67	−0.99
3	2470	0.018683	0.000307	0.281028	0.000023	−61.7	0.8	−6.8	0.8	3037	3390	68	−0.99
4	2467	0.016651	0.000264	0.281004	0.000024	−62.5	0.8	−7.7	0.8	3065	3439	69	−0.99
5	2450	0.018231	0.000301	0.281062	0.000024	−60.5	0.9	−6.1	0.9	2991	3328	67	−0.99
6	2449	0.034320	0.000598	0.281079	0.000021	−59.9	0.7	−6.0	0.7	2991	3323	66	−0.98
7	2482	0.015253	0.000248	0.281041	0.000026	−61.2	0.9	−6.0	0.9	3015	3348	67	−0.99
8	2472	0.025468	0.000440	0.281114	0.000025	−58.6	0.9	−3.9	0.9	2933	3217	64	−0.99
9	2391	0.024473	0.000386	0.281067	0.000025	−60.3	0.9	−7.3	0.9	2990	3362	67	−0.99
10	2471	0.041247	0.000719	0.281013	0.000023	−62.2	0.8	−8.0	0.8	3089	3464	69	−0.98
11	2472	0.019677	0.000327	0.281085	0.000021	−59.7	0.7	−4.8	0.8	2963	3268	65	−0.99
12	2443	0.019181	0.000319	0.281096	0.000028	−59.3	1.0	−5.0	1.0	2947	3261	65	−0.99
13	2457	0.016251	0.000266	0.281021	0.000021	−61.9	0.8	−7.3	0.8	3043	3410	68	−0.99
14	2460	0.015995	0.000262	0.281070	0.000022	−60.2	0.8	−5.5	0.8	2978	3301	66	−0.99
15	2487	0.013768	0.000229	0.281095	0.000025	−59.3	0.9	−3.9	0.9	2942	3227	65	−0.99
16	2475	0.017427	0.000274	0.281079	0.000025	−59.9	0.9	−4.8	0.9	2966	3272	65	−0.99
17	2489	0.030582	0.000542	0.281061	0.000025	−60.5	0.9	−5.6	0.9	3010	3330	67	−0.98
18	2482	0.025703	0.000444	0.281073	0.000024	−60.1	0.9	−5.2	0.9	2988	3300	66	−0.99
19	2496	0.039934	0.000711	0.281085	0.000029	−59.7	1.0	−4.9	1.0	2992	3292	66	−0.98
20	2457	0.025578	0.000410	0.281094	0.000024	−59.3	0.9	−4.9	0.9	2957	3266	65	−0.99
21	2492	0.017619	0.000279	0.281060	0.000025	−60.6	0.9	−5.1	0.9	2992	3305	66	−0.99
22	2484	0.016705	0.000260	0.281079	0.000029	−59.9	1.0	−4.6	1.0	2965	3266	65	−0.99
23	2472	0.032328	0.000533	0.281085	0.000022	−59.7	0.8	−5.1	0.8	2978	3289	66	−0.98
24	2468	0.024544	0.000384	0.281195	0.000027	−55.8	0.9	−1.0	0.9	2820	3038	61	−0.99
Sample XP08-4 (amphibole-plagioclase gneiss)													
1	2477	0.032853	0.000528	0.281237	0.000028	−54.3	1.0	0.4	1.0	2774	2956	59	−0.98
2	2480	0.022198	0.000352	0.281263	0.000024	−53.4	0.9	1.7	0.9	2726	2879	58	−0.99
3	2486	0.022592	0.000350	0.281174	0.000026	−56.5	0.9	−1.3	0.9	2845	3069	61	−0.99
4	2495	0.037288	0.000580	0.281277	0.000023	−52.9	0.8	2.1	0.8	2724	2864	57	−0.98
5	2490	0.015181	0.000248	0.281262	0.000029	−53.4	1.0	2.1	1.0	2720	2865	57	−0.99
6	2491	0.031697	0.000470	0.281222	0.000030	−54.8	1.1	0.3	1.1	2790	2975	59	−0.99
8	2491	0.016426	0.000250	0.281229	0.000030	−54.6	1.1	0.9	1.1	2765	2937	59	−0.99
9	2503	0.020472	0.000295	0.281224	0.000029	−54.7	1.0	0.9	1.1	2774	2944	59	−0.99
10	2487	0.028369	0.000495	0.281266	0.000025	−53.2	0.9	1.7	0.9	2732	2883	58	−0.99
11	2463	0.030810	0.000468	0.281211	0.000030	−55.2	1.0	−0.7	1.1	2804	3015	60	−0.99
12	2503	0.019421	0.000284	0.281120	0.000029	−58.4	1.0	−2.7	1.0	2912	3167	63	−0.99
13	2485	0.033318	0.000495	0.281188	0.000030	−56.0	1.0	−1.1	1.1	2837	3054	61	−0.99
14	2429	0.035425	0.000501	0.281255	0.000031	−53.6	1.1	0.0	1.1	2747	2943	59	−0.98
15	2410	0.021646	0.000332	0.281172	0.000027	−56.6	1.0	−3.1	1.0	2847	3118	62	−0.99
16	2407	0.023619	0.000386	0.281236	0.000028	−54.3	1.0	−1.0	1.0	2765	2986	60	−0.99
17	2466	0.034448	0.000521	0.281183	0.000027	−56.2	1.0	−1.8	1.0	2846	3079	62	−0.98
18	2497	0.030782	0.000493	0.281262	0.000025	−53.4	0.9	1.8	0.9	2739	2887	58	−0.99

(*To be continued on the next page*)

(*Continued*)

Spot	t (Ma)	$^{176}Yb/^{177}Hf$	$^{176}Lu/^{177}Hf$	$^{176}Hf/^{177}Hf$	2σ	$\varepsilon_{Hf}(0)$	2σ	$\varepsilon_{Hf}(t)$	2σ	T_{Hf1}	T_{Hf2}	2σ	$f_{Lu/Hf}$
19	2477	0.028780	0.000525	0.281256	0.000025	−53.6	0.9	1.1	0.9	2747	2914	58	−0.98
20	2495	0.017825	0.000300	0.281222	0.000026	−54.8	0.9	0.7	0.9	2778	2955	59	−0.99
21	2501	0.025564	0.000405	0.281329	0.000030	−51.0	1.1	4.4	1.1	2642	2730	55	−0.99
22	2512	0.026609	0.000372	0.281283	0.000029	−52.7	1.0	3.1	1.1	2702	2820	56	−0.99
23	2360	0.040239	0.000678	0.281285	0.000029	−52.6	1.0	−0.8	1.0	2720	2938	59	−0.98
24	2490	0.021345	0.000325	0.281177	0.000030	−56.4	1.1	−1.1	1.1	2839	3056	61	−0.99
Sample XP16-4 (two-feldspar gneiss)													
1	2448	0.021376	0.000355	0.281109	0.000019	−58.8	0.7	−4.5	0.7	2933	3234	65	−0.99
2	2481	0.055966	0.000826	0.281122	0.000023	−58.4	0.8	−4.1	0.8	2951	3234	65	−0.98
3	2473	0.054215	0.000827	0.281130	0.000022	−58.1	0.8	−4.0	0.8	2940	3221	64	−0.98
4	2448	0.013662	0.000198	0.281098	0.000023	−59.2	0.8	−4.6	0.8	2935	3241	65	−0.99
5	2490	0.048603	0.000750	0.281125	0.000019	−58.2	0.7	−3.6	0.7	2940	3213	64	−0.98
6	2479	0.071112	0.001034	0.281193	0.000025	−55.8	0.9	−2.0	0.9	2870	3102	62	−0.97
7	2556	0.025717	0.000373	0.281161	0.000023	−57.0	0.8	−0.2	0.8	2865	3056	61	−0.99
8	2482	0.031154	0.000493	0.281174	0.000021	−56.5	0.7	−1.7	0.8	2856	3086	62	−0.99
9	2465	0.041580	0.000637	0.281114	0.000021	−58.6	0.7	−4.4	0.8	2947	3240	65	−0.98
10	2493	0.044124	0.000678	0.281114	0.000024	−58.7	0.9	−3.9	0.9	2951	3229	65	−0.98
11	2489	0.040146	0.000596	0.281133	0.000023	−58.0	0.8	−3.1	0.8	2919	3182	64	−0.98
12	2493	0.025713	0.000400	0.281078	0.000020	−59.9	0.7	−4.7	0.7	2978	3278	66	−0.99
13	2140	0.033456	0.000478	0.281154	0.000023	−57.2	0.8	−10.1	0.8	2881	3338	67	−0.99
14	2517	0.026889	0.000380	0.281120	0.000021	−58.4	0.7	−2.6	0.8	2920	3170	63	−0.99
15	2440	0.012678	0.000164	0.281154	0.000018	−57.2	0.6	−2.8	0.7	2859	3122	62	−1.00
16	2507	0.042581	0.000660	0.281168	0.000024	−56.7	0.9	−1.6	0.9	2876	3101	62	−0.98
17	2507	0.051781	0.000776	0.281091	0.000021	−59.4	0.8	−4.5	0.8	2988	3279	66	−0.98
18	2494	0.039142	0.000549	0.281123	0.000025	−58.3	0.9	−3.3	0.9	2928	3195	64	−0.98
19	2551	0.021280	0.000316	0.281089	0.000024	−59.5	0.9	−2.8	0.9	2957	3209	64	−0.99
20	2497	0.095047	0.001545	0.281172	0.000025	−56.6	0.9	−3.2	0.9	2937	3189	64	−0.95
21	2484	0.030754	0.000407	0.281108	0.000028	−58.8	1.0	−3.8	1.0	2937	3218	64	−0.99
22	2548	0.084196	0.001230	0.281172	0.000034	−56.6	1.2	−1.5	1.2	2914	3128	63	−0.96
23	2677	0.045407	0.000682	0.281108	0.000026	−58.8	0.9	0.1	0.9	2958	3129	63	−0.98
24	2440	0.028683	0.000384	0.281133	0.000027	−58.0	0.9	−3.9	1.0	2903	3190	64	−0.99
Sample SN07-7 (biotite-plagioclase gneiss)													
1	2500	0.090779	0.001374	0.281137	0.000030	−57.8	1.1	−4.1	1.1	2973	3246	65	−0.96
2	2482	0.075692	0.001225	0.281112	0.000029	−58.7	1.0	−5.1	1.0	2995	3294	66	−0.96
3	2507	0.094154	0.001510	0.281184	0.000030	−56.2	1.0	−2.5	1.1	2918	3154	63	−0.95
4	2517	0.059971	0.000980	0.281139	0.000024	−57.8	0.8	−3.0	0.8	2940	3191	64	−0.97
5	2488	0.053508	0.000896	0.281101	0.000024	−59.1	0.9	−4.8	0.9	2985	3282	66	−0.97
6	2594	0.062166	0.001013	0.281142	0.000029	−57.6	1.0	−1.2	1.0	2938	3142	63	−0.97
7	2621	0.079245	0.001233	0.281213	0.000025	−55.1	0.9	1.6	0.9	2858	2997	60	−0.96
8	2591	0.056336	0.000872	0.281093	0.000029	−59.4	1.0	−2.7	1.0	2994	3235	65	−0.97
9	2326	0.052819	0.000838	0.281094	0.000030	−59.3	1.1	−8.6	1.1	2990	3388	68	−0.97
10	2601	0.067603	0.001046	0.281118	0.000030	−58.5	1.1	−1.9	1.1	2973	3193	64	−0.97
11	2549	0.104729	0.001613	0.281128	0.000033	−58.1	1.2	−3.7	1.2	3004	3263	65	−0.95
12	2495	0.077989	0.001221	0.281204	0.000028	−55.5	1.0	−1.5	1.0	2869	3088	62	−0.96
13	2588	0.084612	0.001308	0.281169	0.000028	−56.7	1.0	−0.9	1.0	2923	3118	62	−0.96
14	2628	0.044381	0.000704	0.281120	0.000028	−58.4	1.0	−0.6	1.0	2944	3135	63	−0.98
15	2618	0.030453	0.000468	0.281164	0.000030	−56.8	1.1	1.1	1.1	2867	3020	60	−0.99
16	2496	0.097605	0.001651	0.281182	0.000029	−56.2	1.0	−3.0	1.0	2932	3179	64	−0.95
17	2621	0.088135	0.001506	0.281225	0.000026	−54.7	0.9	1.5	0.9	2862	3000	60	−0.95
18	2550	0.019182	0.000336	0.281121	0.000025	−58.4	0.9	−1.7	0.9	2915	3142	63	−0.99
19	2630	0.086871	0.001493	0.281175	0.000029	−56.5	1.0	0.0	1.0	2929	3101	62	−0.96
20	2681	0.104564	0.001735	0.281126	0.000029	−58.2	1.0	−1.1	1.0	3016	3205	64	−0.95
21	2449	0.141418	0.002151	0.281245	0.000030	−54.0	1.1	−2.7	1.1	2884	3121	62	−0.94
22	2616	0.086947	0.001308	0.281129	0.000031	−58.1	1.1	−1.7	1.1	2978	3189	64	−0.96
23	2620	0.126818	0.001860	0.281219	0.000030	−54.9	1.1	0.6	1.1	2898	3053	61	−0.94
24	2598	0.117275	0.001791	0.281224	0.000031	−54.8	1.1	0.5	1.1	2885	3046	61	−0.95

in length and length to width ratios of 1:1–2.5:1. Cathodoluminescence images reveal that most zircon grains show distinct oscillatory zonation (Figure 3(a)). Some zircon grains display grey metamorphic overgrowth rims (Figure 3(b)). Twenty-four spot analyses on 22 zircon grains were performed on this sample, including 18 oscillatory-zoned cores and 6 overgrowth rims. Except for 2 analyses that are slightly discordant, 16 analyses from oscillatory-zoned cores yield a discordia line with an upper intercept age of 2469 ± 22 Ma and a lower intercept age of 973 ± 37 Ma (MSWD = 3.6) (Figure 4(a)). These oscillatory-zoned cores show U contents of 31–710 ppm and Th contents of 4–191 ppm, with Th/U ratios ranging from 0.07 to 0.90. Among the 6 grey zircon overgrowth rim analyses, 4 analyses are concordant and tightly grouped, yielding a weighted mean $^{206}Pb/^{238}Pb$ age of 837 ± 8 Ma (MSWD = 0.33). These analyses have U concentrations of 71–362 ppm and Th concentrations of 0.3–132 ppm, with Th/U ratios of 0.01–0.09, indicating that these zircon rims are typically of metamorphic origin. The remaining 2 older data are highly discordant and may have no geological meaning. Therefore, the upper intercept age of 2469 ± 22 Ma is taken to be the protolith age of amphibole-plagioclase gneiss, whereas the concordant age of 837 ± 8 Ma could be interpreted as the metamorphic age.

3.2 Amphibole-plagioclase gneiss (sample XX43-2)

The zircons from the amphibole-plagioclase gneiss sample XX43-2 are ovoid to prismatic in shape, with grain sizes of 80–300 μm and aspect ratios of 1.5:1–3:1. Most grains are characterized by an oscillatory-zoned core and a narrow, strongly luminescent rim (<10 μm) (Figure 3(c)). Some zircon grains show grey planar zoning. Twenty-four spot analyses on 24 zircons are tightly clustered, yielding an upper and a lower intercept ages of 2479 ± 12 Ma and 798 ± 330 Ma, respectively (MSWD = 0.62) (Figure 4(b)). The weighted mean $^{207}Pb/^{206}Pb$ age of 2469 ± 8 Ma (MSWD = 1.11) obtained for these analyses is in agreement within error with the upper intercept age of 2479 ± 12 Ma. These zircon grains have U abundances of 28–303 ppm and Th abundances of 34–156 ppm with Th/U ratios ranging from 0.59 to 1.88, indicating their magmatic origin. Therefore, the upper intercept age of 2479 ± 12 Ma is interpreted as the protolith age of the amphibole-plagioclase gneiss.

3.3 Plagioclase gneiss (sample XP08-4)

The zircons from the plagioclase gneiss sample XP08-4 are ovoid to prismatic in shape, with 100–300 μm in length and aspect ratios of 1.5:1–3:1. Most of them have an oscillatory-zoned core or grey homogeneous core. In most cases, an inhomogeneously luminescent rim is discontinuously developed and too thin to be analyzed (Figure 3(d)), representing growth in the late stage. Twenty-four spot analyses form a discordia line with an upper intercept age of 2497 ± 21 Ma and a lower intercept age of 431 ± 280 Ma (MSWD = 2.6) (Figure 4(c)). A weighted mean $^{207}Pb/^{206}Pb$ age of 2479 ± 10 Ma (MSWD = 1.5) is obtained for the same analyses, which is roughly coincident within error with the upper intercept age of 2497 ± 21 Ma. These zircons have U contents of 47–279 ppm and Th contents of 31–275 ppm, with Th/U ratios ranging from 0.13 to 5.61. The upper intercept age of 2497 ± 21 Ma is interpreted as the for-

Figure 3 Representative cathodoluminescence (CL) images of zircons from the Douling Complex. The white circles show spots for U-Pb analyses. The diameter of white circles is 35 μm.

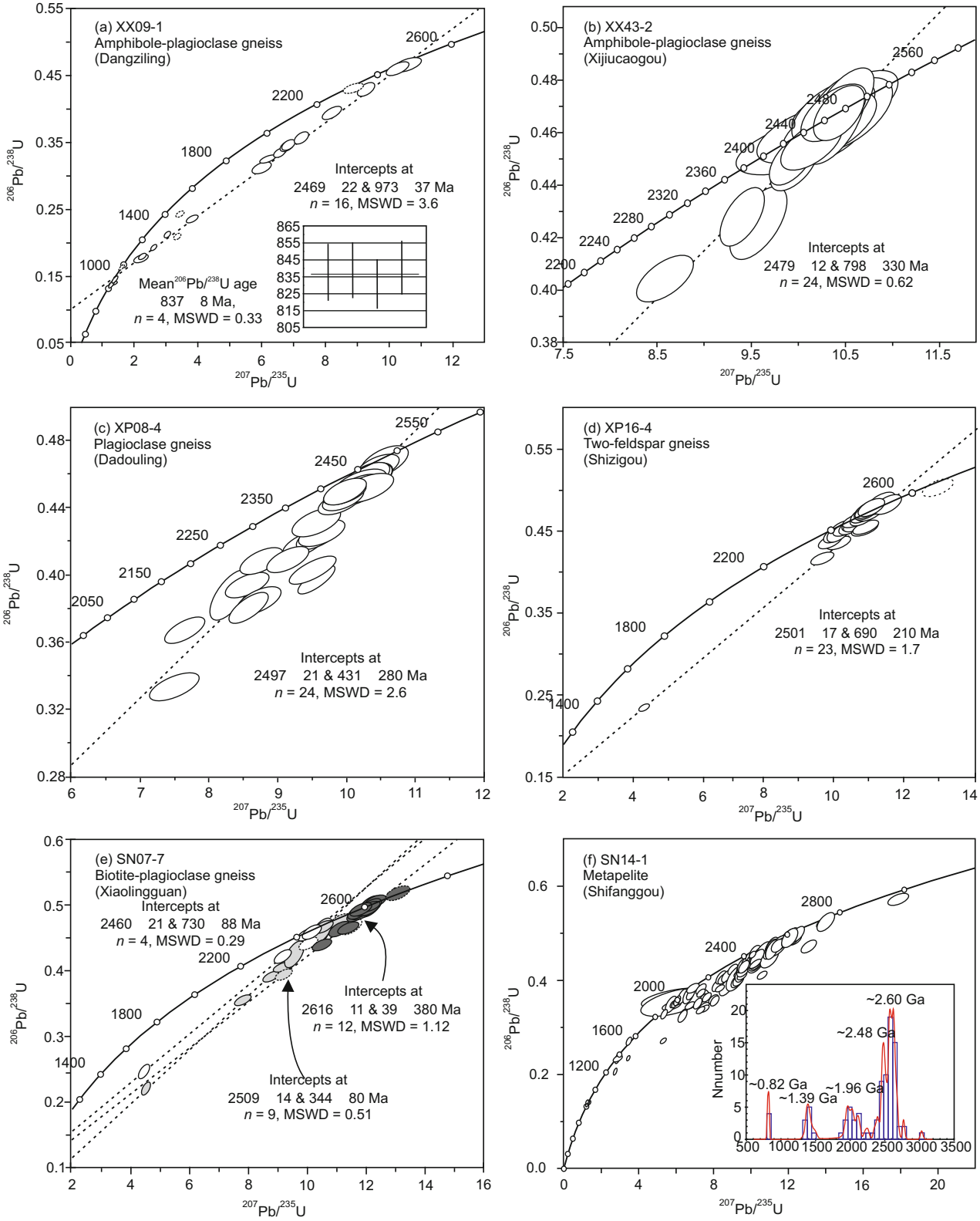

Figure 4 Zircon U-Pb concordia diagrams of the dioritic-granitic gneisses from the Douling Complex.

mation age of plagioclase gneiss protolith.

3.4 Two-feldspar gneiss (sample XP16-4)

The zircons from the two-feldspar gneiss sample XP16-4 are ovoid to prismatic in shape, with grain sizes ranging from 120 to 260 μm and aspect ratios of 1.5∶1–3∶1. All of them display a very dark oscillatory-zoned core and a bright or grey narrow luminescent rim (Figure 3(e)). Among 24 spot analyses, 23 spots plot roughly on or near the concor-

dia, which defines a discordant array with an upper intercept age of 2501 ± 17 Ma and a lower intercept age of 690 ± 210 Ma (MSWD = 1.7) (Figure 4(d)). These analyses (except for one with remarkable Pb loss) yield a weighted mean $^{207}Pb/^{206}Pb$ age of 2490 ± 14 Ma (MSWD = 2.0). Zircon grains have high U abundances of 319–1511 ppm and Th abundances of 90–296 ppm, with Th/U ratios of 0.09–0.55. The upper intercept age of 2501 ± 17 Ma is thus considered as the formation age of the two-feldspar gneiss protolith. Another older age of 2677 ± 23 Ma may represent the age of inherited zircons.

3.5 Biotite-plagioclase gneiss (sample SN07-7)

The zircons from the biotite-plagioclase gneiss sample SN07-7 are ovoid to prismatic in shape, with 70–200 μm in length and aspect ratios of 1.5∶1–3∶1. All zircon grains exhibit an oscillatory-zoned core and a narrow, strongly luminescent rim (Figure 3(f)). Some grains develop a wider grey mantle (Figure 3(g)). Thirty spot analyses on 30 zircons are carried out for this sample, including 24 oscillatory-zoned cores and 6 zircon mantles. Among the 24 analyzed cores, except for 3 analyses slightly away from the discordia, 12 analyses define a discordant array with an upper intercept age of 2611 ± 11 Ma and a lower intercept age of 393 ± 380 Ma (MSWD = 1.12, Th/U = 0.03–0.92) (Figure 4(e)). The upper intercept age is in accordance within error with the weighted mean $^{207}Pb/^{206}Pb$ age of 2611 ± 12 Ma (MSWD = 0.51) obtained for the same analyses. The remaining 9 analyses yield a discordia line with an upper intercept age of 2509 ± 14 Ma and a lower intercept age of 344 ± 81 Ma (MSWD = 0.51, Th/U = 0.13–0.43). The weighted mean $^{207}Pb/^{206}Pb$ age of 2503 ± 22 Ma (MSWD = 2.1) obtained for the same analyses is in agreement within error with the upper intercept age. Of the 6 gray mantle analyses, except for 2 slightly discordant spots, 4 analyses form a discordant array with intercept ages of 2460 ± 21 Ma and 730 ± 88 Ma (MSWD = 0.29, Th/U = 0.38–1.26). It is inferred that the zircon core age of 2509 ± 14 Ma reflects the magmatic emplacement age of the biotite-plagioclase gneiss protolith, whereas age of 2611 ± 11 Ma may be inherited age, and the zircon mantle age of 2460 ± 21 Ma represents the timing of a tectonothermal event.

3.6 Metapelite (sample SN14-1)

For the metapelite sample SN14-1, 120 detrital zircon grains were randomly dated. The U-Pb zircon ages with <95% concordance are rejected in constructing the age probability density diagrams. For zircon ages ⩾1.0 Ga, the $^{207}Pb/^{206}Pb$ age is used in our interpretation, whereas for ages <1.0 Ga, the $^{206}Pb/^{238}U$ age is used. All zircons are rounded or ovoid to prismatic in shape, with 40–160 μm in length and aspect ratios of 1∶1–3.5∶1. The majority of zircons show oscillatory zonation (Figure 3(h),(i)) and some have homogeneous grey color. Most of them are of magmatic origin. These zircons commonly contain a narrow overgrowth rim, but some grains have a wider overgrowth rim, which, in some cases, also occurs as individual grains. These zircon domains are sector-zoned, indicative of metamorphic origin (Figure 3(j)). One hundred and sixteen spot analyses were conducted on 116 zircon grains with oscillatory zonation or grey domains. The U-Pb zircons ages with >95% concordance yielded an age range from 3032 ± 19 Ma to 1362 ± 23 Ma. Two major age peaks are found at ~2.60 and ~2.48 Ga, and two subordinate age populations at ~1.96 and ~1.39 Ga (Figure 4(f)). Only spot 52 (1956 ± 18 Ma) and two other spots (spot 34, 1973 ± 215 Ma; spot 58, 1982 ± 200 Ma) with large error are of metamorphic origin. The remaining 4 spots, either located in sector-zoned rims or individual grains, yielded a weighted mean $^{206}Pb/^{238}U$ age of 818 ± 10 Ma (MSWD = 0.82). Their Th/U ratios range from 0.01 to 0.02, further suggesting a metamorphic origin for them.

4 Hf isotopic results

All 4 samples have $^{176}Lu/^{177}Hf$ ratios varying from 0.0002 to 0.0022 and $^{176}Hf/^{177}Hf$ ratios from 0.281004 to 0.281329. The calculated initial $^{176}Hf/^{177}Hf$ ratios ($\varepsilon_{Hf}(t)$) and two-stage Hf model ages (T_{Hf2}) are as follows: $\varepsilon_{Hf}(t)$ from −8.0 to −1.1 (average −5.5) and T_{Hf2} = 3464–3038 Ma (weighed mean 3303 ± 37 Ma, MSWD = 1.7 for sample XX43-2 (Figure 5(a), (b)); $\varepsilon_{Hf}(t)$ from −3.1 to 4.4 (average 0.3) and T_{Hf2} = 3167-2730 Ma (weighed mean 2951 ± 44 Ma, MSWD = 3.0) for sample XP08-4 (Figure 5(c), (d)); $\varepsilon_{Hf}(t)$ from −10.1 to 0.1 (average −3.4) and T_{Hf2} = 3338-3056 Ma (weighted mean 3188 ± 29 Ma, MSWD=1.16) for sample XP16-4 (Figure 5(e),(f)); $\varepsilon_{Hf}(t)$ from −8.6 to 1.6 (average −1.9) and T_{Hf2} = 3338–2997 Ma (weighted mean 3152 ± 41 Ma, MSWD = 2.4) for sample SN07-7 (Figure 5(g),(h)).

5 Discussion and conclusions

It is generally accepted that the Kongling Group exposed in the Huangling antiform is representative of the old crystalline basement of the Yangtze craton. The oldest emplacement age of ~2.95–2.9 Ga in the Kongling Group comes from TTG gneisses of the high grade metamorphic terrane [15–17,19,20]. The 3.3–3.2 Ga inherited zircon cores are also present from the same area, and some tonalite gneisses possibly intruded in the terrane during the same period [18]. Chen et al.[20] recently identified emplacement ages of 2.7–2.6 Ga for A-type granites, which is similar to the age of 2693 ± 9 Ma obtained for the granite intrusion of the Yudongzi Group [21] and the protolith age of 2.75–2.70 Ga reported for the Huangluling granulite in the Dabie Mountain [22,23]. In fact, the age data of these three groups were

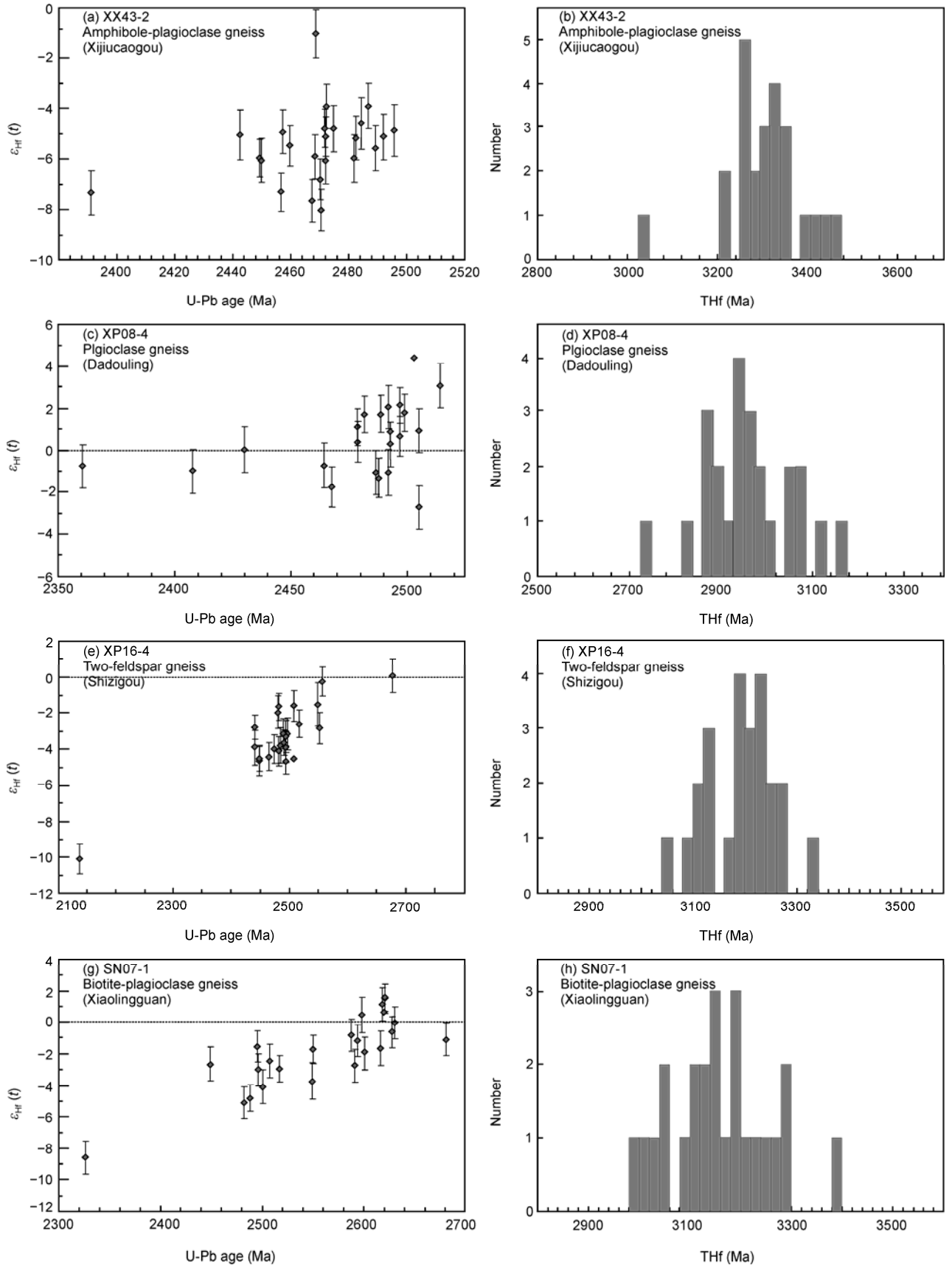

Figure 5 Zircon $\varepsilon_{Hf}(t)$ value vs U-Pb age diagram and Hf model age histogram of the dioritic-granitic gneisses from the Douling Complex.

also recorded in detrital zircons from metasedimentary rocks [5–9] and inherited zircons from igneous rocks [10–14] in different areas of the Yangtze craton, suggesting that the 3.3–3.2 Ga, 2.95–2.9 Ga and 2.7–2.6 Ga eras are important periods for the continental crustal growth in the Yangtze craton.

In this paper, detrital zircon age of ~2.6 Ga and inherited zircon age of 2616 ± 11 Ma are also identified in the Douling Complex, further confirming the presence of the 2.7–2.6 Ga igneous event in the Yangtze craton. Most importantly, the tightly clustered protolith ages of 2469 ± 22 Ma, 2479 ± 12 Ma, 2497 ± 21 Ma, 2501 ± 17 Ma and 2509 ± 14 Ma were obtained for five dioritic-granitic gneisses, and an important peak age of ~2.48 Ga was also obtained for a metasedimentary rock. Similar age data were formerly reported in the Dabie-Sulu region. For example, the crystallization age of 2493 ± 13 Ma [38] was obtained for the TTG gneiss underlying the Zhangbaling Group in the eastern Anhui province, and the upper intercept age of 2458 ± 76 Ma [39] was recorded in zircon from the Shuanghe gneiss in the Dabie Mountain. Also in the Dabie Mountains, Chen et al. [40] reported another upper intercept zircon age of 2489 ± 25 Ma from an eclogite. Moreover, a remarkable peak age of ~2.49 Ga was found in detrital zircons at the northern margin of the Yangtze craton [7,8]. All these geochronology results suggest the occurrence of an igneous event of 2.51–2.47 Ga at the northern margin of the Yangtze craton. Although a grey zircon mantle age of 2460 ± 21 Ma is obtained for sample SN07-7, whether it represents an early Paleoproterozoic metamorphic event needs to be further studied.

The limited geochemical analytical results show that dioritic-granitic gneisses of the Douling Complex have the characteristics of the TTG compositions [28]. In the present study, zircons from four samples almost have negative $\varepsilon_{Hf}(t)$ value with average values ranging from −5.5 to +0.3, and the corresponding two-stage Hf model ages vary from 3.30 to 2.95 Ga, which are coincident with the two former periods of igneous events in the Yangtze craton. It can be hence inferred that the compostions of the 2.5 Ga TTG gneisses from the Douling Complex are mainly reworked from the Paleo- to Mesoarchean crust at the northern margin of theYangtze craton. There may be a small contribution from juvenile materials.

In addition, the geochronological data on the Douling Complex has also provided two other important informations. Firstly, detrital zircons from a metasedimentary rock show two peak ages of ~1.96 and ~1.39 Ga, suggesting that the Yangtze craton not only experienced Paleoproterozoic reworking and Neoproterozoic continental crustal growth [4], but also underwent Mesoproterozoic magmatic activity whose nature needs to be further determined. Secondly, the metamorphic ages of 837 ± 8 Ma and 818 ± 10 Ma on zircon overgrowth rims are obtained from a dioritic gneiss and a metasedimentary rock, which are similar to the metamorphic zircon age of 834 ± 31 Ma for a calc-silicate rocks reported by Zhang et al. [28] and also the amphibole $^{40}Ar/^{39}Ar$ age of 818 ± 10 Ma obtained for amphibolite by Shen et al. [29]. This indicates that the main phase amphibolite facies metamorphism of the Douling Complex occurred during the Neoproterozoic, which is still unreported for the Yangtze craton. The more recent research indicates that widespread arc magmatism related to oceanic subduction may have occurred at the northern margin of the Yantze craton [41,42]. However, it is unclear whether this metamorphism is associated with this accretionary orogenic event.

We are grateful to Hou Kejun for his help during the LA-MC-ICP-MS zircon Hf isotopic analyses. Critical reviews by two anonymous reviewers and editorial comments by Prof. Zhao Guochun substantially improved the manuscript. This work was supported by the National Basic Research Program of China (2009CB825006).

1 Zheng Y F. A perspective view on ultrahigh-pressure metamorphism and continental collision in the Dabie-Sulu orogenic belt. Chin Sci Bull, 2008, 53: 3081–3104
2 Zhai M G, Li T S, Peng P, et al. Precambrian key tectonic events and evolution of the North China craton. In: Kusky T M, Zhai M G, Xiao W J, eds. The Evolving Continents. Geol Soc Lond Spec Pub, 2010, 338: 235–262
3 Zhao G C, Cawood P A. Precambrian geology of China. Precambrian Res, 2012, 222-223: 13–54
4 Zheng Y F, Zhang S B. Formation and evolution of Precambrian continental crust in South China. Chin Sci Bull, 2007, 52: 1–12
5 Liu X M, Gao S, Ling W L, et al. Identification of 3.5 Ga detrital zircons from Yangtze craton in south China and the implication for Archean crust evolution. Prog Nat Sci, 2006, 16: 663–666
6 Zhang S B, Zheng Y F, Wu Y B, et al. Zircon U-Pb age and Hf isotope evidence for 3.8 Ga crustal remnant and episodic reworking of Archean crust in South China. Earth Planet Sci Lett, 2006, 252: 56–71
7 Liu X M, Gao S, Diwu C R, et al. Precambrian crustal growth of Yangtze Craton as revealed by detrital zircon studies. Am J Sci, 2008, 308: 421–468
8 Liu X C, Jahn B M, Dong S W, et al. High-pressure metamorphic rocks from Tongbaishan, central China: U-Pb and $^{40}Ar/^{39}Ar$ age constraints on the provenance of protoliths and timing of metamorphism. Lithos, 2008, 105: 301–318
9 Ling W L, Duan R C, Liu X M, et al. U-Pb dating of detrital zircons from the Wudangshan Group in the South Qinling and its geological significance. Chin Sci Bull, 2010, 55: 2440–2448
10 Ma G G, Li H Q, Zhang Z C, et al. An investigation of the age limits of the Sinian System in South China (in Chinese). Yichang Inst Geol Miner Resour Bull, 1984, 8: 1–29
11 Zhang Q, Jian P, Liu D Y, et al. SHRIMP dating of volcanic rocks from Ningwu area and its geological implications. Sci China Ser D-Earth Sci, 2003, 46: 830–837
12 Liu H Y, Xia B, Zhang Y Q. Zircon SHRIMP dating of sodium alkaline rocks from Maomaogou area of Huili County in Panxi, SW China and its geological implications. Chin Sci Bull, 2004, 49: 1750–1756
13 Chen Y L, Luo Z H, Zhao J X, et al. Petrogenesis and dating of the Kangding complex, Sichuan Province. Sci China Ser D-Earth Sci, 2005, 48: 622–634
14 Zheng J P, Griffin W L, O'Reilly S Y, et al. Widespread Archean basement beneath the Yangtze craton. Geology, 2006, 34: 417–420
15 Gao S, Ling W, Qiu Y, et al. Contrasting geochemical and Sm-Nd isotopic compositions of Archean metasediments from the Kongling high-grade terrain of the Yangtze craton: Evidence for cratonic evolution and redistribution of REE during crustal anatexis. Geochim

Cosmochim Acta, 1999, 63: 2071–2088
16 Qiu Y M, Gao S, McNaughton, et al. First evidence of >3.2 Ga continental crust in the Yangtze craton of south China and its implications for Archean crustal evolution and Phanerozoic tectonics. Geology, 2000, 28: 11–14
17 Zhang S B, Zheng Y F, Wu Y B, et al. Zircon isotope evidence for ⩾3.5 Ga continental crust in the Yangtze craton of China. Precambrian Res, 2006, 146: 16–34
18 Jiao W F, Wu Y B, Yang S H, et al. The oldest basement rock in the Yangtze Craton revealed by zircon U-Pb age and Hf isotope compositon. Sci China Ser D-Earth Sci, 2009, 52: 1393–1399
19 Gao S, Yang J, Zhou L, et al. Age and growth of the Archean Kongling terrain, South China, with emphasis on 3.3 Ga granitoid gneisses. Am J Sci, 2011, 311: 153–182
20 Chen K, Gao S, Wu Y B, et al. 2.6-2.7 Ga crustal growth in Yangtze craton, South China. Precambrian Res, 2013, 224: 472–490
21 Zhang Z Q, Zhang G W, Tang S H, et al. On the age of metamorphic rocks of the Yudongzi group and the Archean crystalline basement of the Qinling orogen. Acta Geol Sin, 2001, 75: 198–204
22 Sun M, Chen N S, Zhao G C, et al. U-Pb zircon and Sm-Nd isotopic study of the Huangtuling granulite, Dabie-Sulu belt, China: Implication for the Paleoproterozoic tectonic history of the Yangtze Craton. Am J Sci, 2008, 308: 469–483
23 Wu Y B, Zheng Y F, Gao S, et al. Zircon U–Pb age and trace element evidence for Paleoproterozoic granulite-facies metamorphism and Archean crustal rocks in the Dabie Orogen. Lithos, 2008, 101: 308–322
24 Zhang G W, Zhang B R, Yuan X C, et al. Qinling Orogenic Belt and Continental Dynamics (in Chinese). Beijing: Science Press, 2001. 1–855
25 Dong Y P, Zhang G W, Neubauer F, et al. Tectonic evolution of the Qinling orogen, China: Review and synthesis. J Asian Earth Sci, 2011, 41: 213–237
26 Wu Y B, Zheng Y F. Tectonic evolution of a composite collision orogen: An overview on the Qinling-Tongbai-Hong'an-Dabie-Sulu orogenic belt in central China. Gondwana Res, 2013, 23: 1402–1428
27 Wei C J, Zhao Z R, Zhang S G. Metamorphism and its geological significance of the Douling Group from the Qinling orogenic belt (in Chinese). In: Lithospheric, Geoscience. Beijing: Seismological Press, 1994. 97–104
28 Zhang S G, Wei C J, Zhao Z R, et al. Formation and metamorphic evolution of the Douling complex from the East Qinling Mountains. Sci China Ser D-Earth Sci, 1996, 39 (Suppl): 80–86
29 Shen J, Zhang Z Q, Liu D Y. Sm-Nd, Rb-Sr, $^{40}Ar/^{39}Ar$, $^{207}Pb/^{206}Pb$ age of the Douling metamorphic complex from Eastern Qinling orogenic belt (in Chinese). Acta Geosci Sin, 1997, 18: 248–254
30 Zhang S G, Zhang Z Q, Song B, et al. On the existence of Neoarchean materials in the Douling complex, Eastern Qinling—Evidence from U-Pb SHRIMP and Sm-Nd geochronology. Acta Geol Sin, 2004, 78: 800–805
31 Li H G, Geng J Z, Hao S, et al. Studies on measuring the U-Pb isotopic age of zircon by using laser ablation multi-collector inductively coupled plasma mass spectrometry (LA-MC-ICPMS) (in Chinese). Acta Mineral Sin, 2009, S1: 600–601
32 Liu Y S, Hu Z C, Gao S, et al. *In situ* analysis of major and trace elements of anhydrous minerals by LA-ICP-MS without applying an internal standard. Chem Geol, 2008, 257: 34–43
33 Liu Y S, Hu Z C, Zong K Q, et al. Reappraisement and refinement of zircon U-Pb isotope and trace element analyses by LA-ICP-MS. Chin Sci Bull, 2010, 55: 1535–1546
34 Ludwig K R. User's Manual for Isoplot 3.00: A geochronological toolkit for Microsoft Excel. Berkeley Geochronological Center Speical Publication, 2003, 4: 70
35 Hou K J, Li Y H, Zou T R, et al. Laser Ablation-MC-ICP-MS technique for Hf isotope microanalysis of zircon and its geological applications (in Chinese). Acta Petrol Sin, 2007, 23: 2595–2603
36 Elhlou S, Belousova E, Griffin W L, et al. Trace element and isotopic composition of GJ-red zircon standard by laser ablation. Geochim Cosmochim Acta, 2006 (Suppl): A158
37 Wu F Y, Li X H, Zheng Y F, et al. Lu-Hf isotope systematics and their applications in petrology (in Chinese). Acta Petrol Sin, 2007, 23: 185–220
38 Tu Y J, Yang X Y, Zheng Y F, et al. U-Pb dating of zircon from gneiss at Nanhuang in East Anhui (in Chinese). Acta Petrol Sin, 2001, 17: 157–160
39 Chavagnac V, Jahn B M, Villa I M, et al. Multichronometric evidence for an *in situ* origin of the ultrahigh pressure metamorphic terrane of Dabieshan, China. J Geol, 2001, 109: 633–646
40 Chen D G, Deloule E, Xia Q K, et al. Metamorphic zircon from Shuanghe ultra-high pressure eclogite, Dabieshan: Ion microprobe and internal micro-structure study (in Chinese). Acta Petrol Sin, 2002, 18: 367–377
41 Dong Y P, Liu X M, Santosh M, et al. Neoproterozoic subduction tectonics of the northwestern Yangtze Block in South China: Constraints from zircon U-Pb geochronology and geochemistry of mafic intrusions in the Hannan Massif. Precambrian Res, 2011, 189: 66–90
42 Dong Y P, Liu X M, Santosh M, et al. Neoproterozoic accretionary tectonics along the northwestern margin of the Yangtze Block, China: Constraints from zircon U-Pb geochronology and geochemistry. Precambrian Res, 2012, 196-197: 247–274